Thermodynamic properties of a tetramer Ising-Heisenberg bond-alternating chain as a model system for $Cu(3\text{-Chloropyridine})_2(N_3)_2$

Jozef Strečka* and Michal Jaščur
Department of Theoretical Physics and Astrophysics, Faculty of Science, P. J. Šafárik University, Park Angelinum 9, 040 01 Košice, Slovak Republic

Masayuki Hagiwara
KYOKUGEN (Research Center for Materials Science at Extreme Conditions), Osaka University, 1-3 Machikaneyama, Toyonaka, Osaka 560-8531, Japan

Kazuhiko Minami
Graduate School of Mathematics, Nagoya University, Nagoya 464-8602, Japan

Yasuo Narumi and Koichi Kindo
Institute for Solid State Physics, University of Tokyo, Kashiwa, Chiba 277–8581, Japan
(Received 28 June 2004; revised manuscript received 1 April 2005; published 26 July 2005)

Thermodynamic properties of a tetramer ferro-ferro-antiferro-antiferromagnetic Ising-Heisenberg bond-alternating chain are investigated by the use of an exact mapping transformation technique. Exact results for the magnetization, susceptibility, and specific heat in zero as well as nonzero magnetic fields are presented and discussed in detail. The results obtained from the mapping are compared with the relevant experimental data of $Cu(3\text{-Clpy})_2(N_3)_2$, where 3-Clpy indicates 3-Chloropyridine.

DOI: 10.1103/PhysRevB.72.024459 PACS number(s): 75.10.Jm, 75.10.Pq

I. INTRODUCTION

Quantum behavior of low-dimensional molecular-based magnetic materials has become one of the most fascinating topics emerging at the border of condensed matter physics, materials science, and inorganic chemistry. In this area, quantum ferrimagnetic chains (QFCs) have attracted considerable attention during the last few years, because they exhibit a remarkable combination of ferromagnetic (F) and antiferromagnetic (AF) features.[1,2] In an attempt directed toward the synthesis and design of possible experimental realizations of a QFC, a magnetostructural analysis of several bimetallic assemblies has been accomplished,[3] since mixed-spin chains afford their most simple and common representatives. Up to now, the dual aspect of QFCs has been experimentally confirmed in the $[NiCu(pba)(D_2O)_3]\cdot 2D_2O$ (Ref. 4) and $[MnCu(mal)_2(H_2O)_4]\cdot 2H_2O$ (Ref. 5) mixed-spin chains, where pba indicates 1,3–propylenebis(oxamato) and mal indicates malonate(2–) ion.

In addition to the mixed-spin chains, another class of QFCs is the bond-alternating chains (BACs) with an unusual fashion of exchanging bonds. From the experimental point of view, the bond alternation in the one-dimensional (1D) polymeric assemblies demands at least two structurally nonequivalent superexchange paths in order to get a series of alternating exchange bonds. It should be mentioned, however, that bond alternation may also arise in a system with a uniform superexchange pathway as a result of the spin-Peierls phenomenon,[6] spontaneous dimerization, which occurs when the elastic energy increase connected with the lattice distortion is lower than the corresponding magnetic energy gain arising from the dimerization. Hence, the recent discovery of the inorganic spin-Peierls compounds $CuGeO_3$ (Ref. 7) and α'-NaV_2O_5 (Ref. 8) gave rise to a number of theoretical works devoted to the spin-1/2 AF-AF BAC.[9]

Another exciting field in molecular magnetism was opened up by Haldane's conjecture,[10] which has already been experimentally verified in several AF nickel-based chains (for a review of Haldane gap compounds see Ref. 11). As first pointed out by Hida,[12] additional insight into the striking properties of the spin-1 AF chain can be acquired by analyzing the spin-1/2 F-AF BAC in the strong-F-coupling limit.[13] Accordingly, much effort has been addressed to prepare polymeric complexes, in which F-AF bond alternation should be realized. At present, there exist several copper-based polymeric compounds that fulfill this requirement[14–20] (see Table I) and Haldane-like behavior has indeed been undoubtedly proved to occur in $(IPA)CuCl_3$.[16]

Of particular interest are also other BACs with more peculiar bond alternation, especially with a longer repeating unit of exchange bonds; namely, according to the Oshikawa-Yamanaka-Affleck rule,[21] one may expect the appearance of the magnetization plateau in any system with a longer period of the ground state. Of course, this rule represents just a necessary condition for the plateau-state formation and does not directly prove its existence in any specific model. The theoretical investigations focused on the magnetization process of the spin-1/2 F-F-AF BAC thus revealed another interesting finding—the breakdown of the magnetization plateau.[22] When the ratio between F and AF coupling constants is strong enough in this system, the plateau state disappears from the magnetization curve. In agreement with this finding, there has not been found any plateau in the low-temperature magnetization curve of $3CuCl_2\cdot 2Dx$,[23] which is

TABLE I. Several examples of one-dimensional copper-based chains with alternating F and AF interactions. TIM indicates 2,3,9,10-tetramethyl-1,3,8,10-tetraenecyclo-1,4,8,11-tetraazatetradecane; 4-BzPip, 4-benzylpiperidinium (1+) ion; IPA, isopropylammonium (1+) ion; DMA, dimethylammonium (1+) ion; bipy, bipyridine; Dx, 1,4-dioxane; Me_2Eten, N,N-dimethyl-N′-ethylethylendiamine; ampy, 1-(2-aminoethyl)pyrrolidine.

Chemical formula	Bond alternation	Reference
$[Cu(TIM)]CuCl_4$	F-AF	14
$(4\text{-BzPip})CuCl_3$	F-AF	15
$(IPA)CuCl_3$	F-AF	16
$(DMA)CuCl_3$	F-AF	17
$[Cu(bipy)(N_3)_2]$	F-AF	18
$[Cu_2(Me_2Eten)_2(N_3)_2](N_3)_2$	F-AF	19
$[Cu_2(ampy)_2(N_3)_2](N_3)_2$	F-AF	20
$3CuCl_2.2Dx$	F-F-AF	23
$Cu(3\text{-Clpy})_2(N_3)_2$	F-F-AF-AF	24

regarded as a typical example of the spin-1/2 F-F-AF BAC with strong F and weak AF coupling.

The versatility of the azido ligand in bridging the magnetic ions in various fashions is nicely demonstrated in the copper-based compound $Cu(3\text{-Clpy})_2(N_3)_2$,[24] where Clpy indicates Chloropyridine, hereafter abbreviated as CCPA. There is a strong evidence that this compound can be regarded as a spin-1/2 tetramer chain with F-F-AF-AF bond alternation.[25–28] However, the 1D nature of the CCPA can be attributed to a sufficient separation between chains, which is ensured by the large steric hindrance of the bulky 3-Clpy ligands [see Fig. 1(a)]. The peculiar F-F-AF-AF sequence of the exchange bonds arises, on the other hand, on account of two kinds of bridging of the azido group: the magnetic Cu^{2+} ions are linked either in a double end-on or in an end-on and end-to-end bridging fashion. It is quite well established[29] that

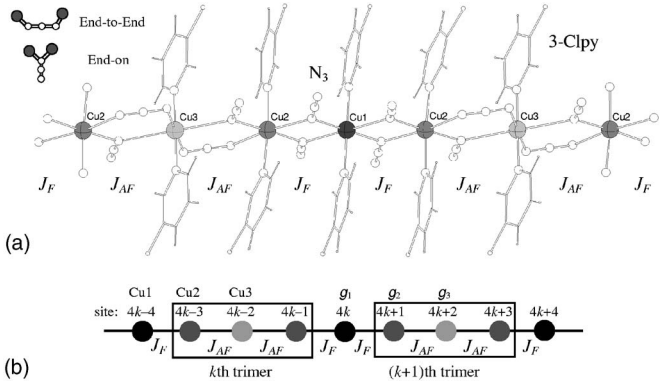

FIG. 1. A fragment of the CCPA structure. (a) shows full details with the azido (N_3) bridges as well as the bulky 3-Clpy ligands; (b) schematically reproduces the considered magnetic structure only. There are three nonequivalent positions of the Cu^{2+} ions: the Cu1 sites coupled purely by the F interaction (black circles), the Cu2 sites coupled via both F and AF interactions (gray circles), and last the Cu3 sites coupled purely by the AF interaction (light gray circles). The rectangles designate the AF trimers.

the end-on bridges are usually associated with the F coupling (with exception when the bridging angle is too large), while the end-to-end bridges are responsible for the AF coupling. Complete magnetic studies of CCPA have been performed by Hagiwara and co-workers: for a powder sample high-field magnetization and the susceptibility measurements were reported,[25] while for a single-crystal sample the high-field magnetization and susceptibility are known,[26] as well as the specific heat[27] and electron-spin resonance[28] data.

The primary purpose of this work is to provide a detailed description of the thermodynamic properties of the spin-1/2 F-F-AF-AF BAC by means of a simplified Ising-Heisenberg model suggested in our preliminary report.[30] Due to the simplicity of the proposed Hamiltonian as well as its low dimensionality, an accurate analytical treatment for the complete set of thermodynamic quantities can be elaborated within an exact mapping transformation technique.[31] To the best of our knowledge, there have been reported only a few rigorous results for the spin-1/2 F-F-AF-AF BAC obtained by applying the exact diagonalization method for a finite-size Heisenberg cluster[25–28] and any further more comprehensive studies have not been reported in the literature hitherto.[32]

The outline of this paper is as follows. In the next section, we shall provide the detailed description of the model system and then the basic ideas of the transformation procedure will be presented. This is followed by the presentation of the most interesting results. An exhaustive survey of results for several thermodynamic quantities in zero as well as nonzero external field is reviewed in Sec. III A, while a comparison with the relevant experimental data is included in Sec. III B. Finally, some concluding remarks are drawn in Sec. IV.

II. MODEL AND METHOD

A fragment of the CCPA crystal structure is depicted in Fig. 1(a). Apparently, there are three nonequivalent positions of the Cu^{2+} ions due to two different kinds of azido bridges. To match the structural situation from the magnetic viewpoint, Fig. 1(b) schematically reproduces the magnetic structure of CCPA: the sites interacting purely via the F interaction J_F are denoted as the Cu1 sites, the sites coupled via both F as well as AF interaction as the Cu2 sites, and finally the sites coupled purely through the AF interaction J_{AF} are labeled as the Cu3 sites. As a consequence of the structural differences, one also has to assume various g factors g_1, g_2, and g_3 at the Cu1, Cu2, and Cu3 sites, respectively.

It is worthwhile to say that the supposed magnetic structure can also be identified as a ferromagnetic chain, the bonds of which are decorated by the AF trimers [Fig. 1(b)]. Owing to this fact, it is very advisable to assume that the F interaction J_F has an Ising-type character, whereas the AF interaction J_{AF} may have the more general form of an anisotropic Heisenberg coupling (the detailed discussion will be given in Sec. III). Under the circumstances, the model under consideration can be exactly treated by applying a generalized decoration-iteration mapping transformation.[30] Actually, this mapping procedure has been proved to be very useful in investigating several mixed-bond Ising-Heisenberg models, some of the present authors already obtained within this

scheme exact results for the trimerized Ising-Heisenberg linear chain,[33] the Ising-Heisenberg diamond chain,[34] and some decorated Ising-Heisenberg planar models.[35] In what follows, we will refer to the Cu1 magnetic sites as to the Ising-type sites, whereas the Cu2 and Cu3 sites will be denoted as the Heisenberg-type sites.

Let us write the total Hamiltonian of the spin-1/2 F-F-AF-AF Ising-Heisenberg chain comprised of $4N$ magnetic sites. By imposing a periodic boundary condition ($S_{4N+1}=S_1$), the total Hamiltonian of the system takes the form

$$H = J_{AF}\sum_{k=1}^{N}[(\mathbf{S}_{4k-3},\mathbf{S}_{4k-2})_{\Delta}+(\mathbf{S}_{4k-2},\mathbf{S}_{4k-1})_{\Delta}] - J_F\sum_{k=1}^{N}[S_{4k-1}^z S_{4k}^z + S_{4k}^z S_{4k+1}^z] - B_1\sum_{k=1}^{N} S_{4k}^z - B_2\sum_{k=1}^{N}(S_{4k-1}^z + S_{4k-3}^z) - B_3\sum_{k=1}^{N} S_{4k-2}^z, \quad (1)$$

where $(\mathbf{S}_i,\mathbf{S}_j)_{\Delta}=\Delta(S_i^x S_j^x+S_i^y S_j^y)+S_i^z S_j^z$, $S_i^{\alpha}(\alpha=x,y,z)$ marks the spatial components of the spin-1/2 operator at the ith lattice point and various on-site magnetic fields $B_j=g_j\mu_B B(j=1,2,3)$ have been introduced in order to distinguish the g factors at the Cu1, Cu2, and Cu3 sites. The first summation accounts for the nearest-neighbor AF Heisenberg coupling ($J_{AF}>0$), Δ is the spatial anisotropy in this interaction, and the second summation accounts for the nearest-neighbor F Ising coupling ($J_F>0$). Other quantities have the usual meaning: μ_B is the Bohr magneton and B the external magnetic field.

For convenience, the total Hamiltonian (1) can be rewritten as a sum of bond Hamiltonians $H=\Sigma_k H_k$, where each bond Hamiltonian H_k involves all the interaction terms associated with the kth AF Heisenberg trimer [Fig. 1(b)]:

$$H_k = J_{AF}[(\mathbf{S}_{4k-3},\mathbf{S}_{4k-2})_{\Delta}+(\mathbf{S}_{4k-2},\mathbf{S}_{4k-1})_{\Delta}] - J_F(S_{4k-4}^z S_{4k-3}^z + S_{4k-1}^z S_{4k}^z) - B_3 S_{4k-2}^z - B_2(S_{4k-1}^z + S_{4k-3}^z) - B_1(S_{4k-4}^z + S_{4k}^z)/2. \quad (2)$$

Obviously, the different bond Hamiltonians commute with respect to each other; hence, the partition function Z can be partially factorized into products of the bond partition functions Z_k:

$$Z = \mathrm{Tr}_{\{4,8,\ldots,4N\}}\prod_{k=1}^{N}\mathrm{Tr}_{\{4k-3,4k-2,4k-1\}}\exp(-\beta H_k),$$

$$Z = \mathrm{Tr}_{\{4,8,\ldots,4N\}}\prod_{k=1}^{N} Z_k. \quad (3)$$

In the above, $\beta=1/(k_B T)$, k_B is Boltzmann's constant, T is the absolute temperature, the symbol $\mathrm{Tr}_{\{4k-3,4k-2,4k-1\}}$ means the trace over the kth AF Heisenberg trimer, and $\mathrm{Tr}_{\{4,8,\ldots,4N\}}$ stands for the trace over the spin states of all Ising-type (Cu1) spins. To proceed further with the calculation, one may introduce at the level of the bond partition function Z_k an extended decoration-iteration transformation by adopting the same idea as already discussed in several papers based on this mapping scheme (see for instance Refs. 33–35):

$$\begin{aligned} Z_k &= \mathrm{Tr}_{\{4k-3,4k-2,4k-1\}}\exp(-\beta H_k) \\ &= \exp[\beta B_1(S_{4k-4}^z + S_{4k}^z)/2] \\ &\quad\times\Bigg\{\exp[\beta(J_{AF}+J_1^+)/6]\sum_{n=1}^{3}\exp(\beta x_n) + \exp[\beta(J_{AF}-J_1^+)/6] \\ &\quad\times\sum_{n=1}^{3}\exp(\beta y_n) + 2\exp(-\beta J_{AF}/2)\cosh(\beta J_1^+/2)\Bigg\} \\ &= A\exp[\beta R S_{4k-4}^z S_{4k}^z + \beta H_0(S_{4k-4}^z + S_{4k}^z)/2]. \end{aligned} \quad (4)$$

Since a complete explicit rendering of the decoration-iteration mapping is in this case rather intricate, we have defined in the transformation Eq. (4) several functions in order to write it in a more appropriate form:

$$J_1^+ = J_F(S_{4k-4}^z + S_{4k}^z) + 2B_2 + B_3, \quad (5)$$

$$J_2^+ = J_F(S_{4k-4}^z + S_{4k}^z) + 2(B_2 - B_3), \quad (6)$$

$$J_1^- = J_F(S_{4k-4}^z - S_{4k}^z), \quad (7)$$

and the terms x_n and y_n denote the roots of two cubic equations that are given as follows:

$$x_n = \pm 2\sqrt{P_1}\cos[\Phi_1 + (n-1)2\pi/3] \quad (n=1,2,3), \quad (8)$$

$$P_1 = [(J_{AF}+J_2^+)/6]^2 + [(J_1^-)^2 + 2(J_{AF}\Delta)^2]/12, \quad (9)$$

$$Q_1 = [(J_{AF}+J_2^+)/6]^3 + [(J_{AF}+J_2^+)/6][(J_{AF}\Delta)^2 - (J_1^-)^2]/4, \quad (10)$$

$$\Phi_1 = \frac{1}{3}\arctan(\sqrt{P_1^3 - Q_1^2}/Q_1); \quad (11)$$

and

$$y_n = \pm 2\sqrt{P_2}\cos[\Phi_2 + (n-1)2\pi/3] \quad (n=1,2,3), \quad (12)$$

$$P_2 = [(J_{AF}-J_2^+)/6]^2 + [(J_1^-)^2 + 2(J_{AF}\Delta)^2]/12, \quad (13)$$

$$Q_2 = [(J_{AF}-J_2^+)/6]^3 + [(J_{AF}-J_2^+)/6][(J_{AF}\Delta)^2 - (J_1^-)^2]/4, \quad (14)$$

$$\Phi_2 = \frac{1}{3}\arctan(\sqrt{P_2^3 - Q_2^2}/Q_2). \quad (15)$$

Note that the signs of x_n and y_n are unambiguously determined by the signs of the expressions Q_1 and Q_2, respectively.

It should be emphasized that the mapping parameters A, R, and H_0 are "self-consistently" given by the transformation Eq. (4), which must be valid for any combination of spin states of the S_{4k-4} and S_{4k} Ising spins. In consequence of that, the mapping parameters can be obtained following the standard procedure[31,33–35] from the expressions

$$A^4 = V_1 V_2 V_3^2, \quad \beta R = \ln(V_1 V_2 / V_3^2), \quad \beta H_0 = \ln(V_1 / V_2), \tag{16}$$

where the functions V_1, V_2, and V_3 have a physical meaning of the bond partition function (4), when taking into account all the particular spin combinations of the S_{4k-4} and S_{4k} Ising spins. These, however, modify merely the effective coupling constants (5)–(7) implicitly contained in Eq. (4). Thus, the functions V_1, V_2, and V_3 are definitely determined by this set of expressions:

$$V_1 = Z_k \text{ if } J_1^+ = J_F + 2B_2 + B_3, \quad J_1^- = 0,$$

$$J_2^+ = J_F + 2(B_2 - B_3), \tag{17}$$

$$V_2 = Z_k \text{ if } J_1^+ = -J_F + 2B_2 + B_3, \quad J_1^- = 0,$$

$$J_2^+ = -J_F + 2(B_2 - B_3), \tag{18}$$

$$V_3 = Z_k \text{ if } J_1^+ = 2B_2 + B_3, \quad J_1^- = J_F,$$

$$J_2^+ = 2(B_2 - B_3). \tag{19}$$

When substituting Eq. (4) into Eq. (3), the transformation Eq. (4) maps the original F-F-AF-AF Ising-Heisenberg BAC on the uniform spin-1/2 Ising chain with the effective nearest-neighbor exchange coupling R and the magnetic field H_0. As a result, the partition function Z of the Ising-Heisenberg BAC can be directly related to the partition function Z_0 of the corresponding Ising chain:

$$Z = A^N Z_0(\beta, R, H_0). \tag{20}$$

Certainly, similar mapping relations can be established also for other thermodynamic quantities. For instance, the Gibbs free energy G of the Ising-Heisenberg BAC can be calculated from the relevant expression of the Gibbs free energy G_0 of the corresponding spin-1/2 Ising chain:

$$G = G_0(\beta, R, H_0) - Nk_B T \ln(A). \tag{21}$$

Since an exact solution for the spin-1/2 Ising chain was known a long time ago,[36] the above equation can serve as the basic generating equation from which all thermodynamic quantities can be extracted. Here, we shall restrict ourselves to the analysis of the magnetization, susceptibility, and specific heat. For the spin-only value of the on-site magnetization at the magnetically nonequivalent Cu1, Cu2, and Cu3 positions, we shall introduce this simple notation:

$$m_1 = \langle \hat{S}_{4k}^z \rangle, \quad m_2 = \langle \hat{S}_{4k-1}^z \rangle, \quad m_3 = \langle \hat{S}_{4k-2}^z \rangle, \tag{22}$$

where the symbol $\langle \cdots \rangle$ stands for a standard canonical average over the ensemble defined by the Hamiltonian (1). In view of this notation, the total magnetization normalized per one Cu^{2+} ion can be expressed as follows: $m = \mu_B(g_1 m_1 + 2g_2 m_2 + g_3 m_3)/4$.

Finally, we briefly mention the basic thermodynamic relations from which all the analyzed quantities have been calculated after straightforward but a little bit lengthy calculations. The on-site magnetization can be obtained by differentiating the Gibbs free energy with respect to the particular magnetic fields:

$$m_1 = -\frac{1}{N}\frac{\partial G}{\partial B_1}, \quad m_2 = -\frac{1}{2N}\frac{\partial G}{\partial B_2}, \quad m_3 = -\frac{1}{N}\frac{\partial G}{\partial B_3}, \tag{23}$$

while the susceptibility and specific heat have been obtained as the second derivatives of the Gibbs potential using the standard thermodynamic relations

$$\chi = -\frac{\partial^2 G}{\partial B^2} \quad \text{and} \quad C = -T\frac{\partial^2 G}{\partial T^2}. \tag{24}$$

It should be stressed that the explicit form for these quantities is too cumbersome to write it down here; however, it can be obtained from the authors on request.

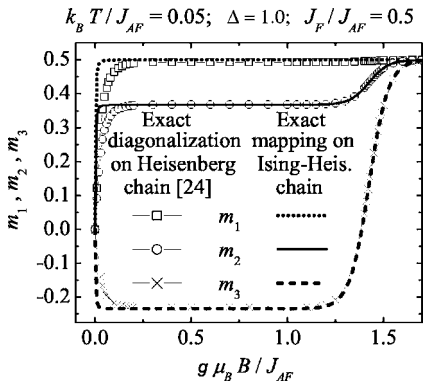

FIG. 2. The comparison between the on-site magnetization of the Ising-Heisenberg BAC and the corresponding pure Heisenberg BAC obtained by the exact diagonalization method as described in Ref. 26. For details see the text.

III. RESULTS AND DISCUSSION

Before proceeding to a discussion of the most interesting results, the model reliability should be checked in connection with its possible application to interpret the experimental data on CCPA, because a danger of overinterpretation is inherent in any approximation. At first glance, we have made in our model a very crude conjecture in that the F interaction J_F was approximated by an Ising-type coupling although all Cu^{2+} ions are nearly isotropic, whence the Heisenberg interaction would be more appropriate. With regard to this, Fig. 2 illustrates a comparison between the on-site magnetization of the Ising-Heisenberg BAC and that of the corresponding pure Heisenberg BAC obtained from the exact diagonalization method for a finite-size cluster of 12 sites.[26] It should be pointed out that the low-temperature ($k_B T/J_{AF}=0.05$) magnetization curve provides the best independent test of the model reliability, since it reflects magnetization near the ground state, where the clearest manifestation of the quantum fluctuations should be expected to occur.

It is quite surprising that there is such an excellent agreement between the two theories: the total magnetization (for clarity not shown here, but see for instance Fig. 4) exhibits a steep increase from zero field followed by a magnetization plateau and finally there appears a second steep increase near

the transition field toward a fully polarized state. Strictly speaking, there is no real phase transition at any finite temperature; however, the low-temperature magnetization curve sheds light on what happens in the ground state: the plateau state should reflect the ground-state phase and a field-induced transition to the fully saturated phase indeed takes place in the zero-temperature limit. Moreover, the magnetic order at the plateau state has the typical feature of a quantum ferrimagnet; in fact, one finds here a substantial quantum reduction of the magnetization m_2 and m_3 at the Cu2 and Cu3 sites even though the magnetization m_1 (Cu1 site) retains its saturation value. It means, among other matters, that the spin deviations cannot propagate through these sites and hence they are strictly localized within the AF trimers. This explains also the remarkable agreement between both the theories, since the quantum fluctuations are in our model artificially restricted to the AF trimers because of the presence of the Ising spins.

The most obvious difference between the magnetization curve of the Ising-Heisenberg BAC and the pure Heisenberg BAC can be thus found in the vicinity of the zero field, where the on-site magnetization of the former reaches its plateau values more rapidly. Apparently, this distinction can be attributed to the more "susceptible" character of the Ising spins, whereby their Heisenberg counterparts achieve the plateau values more rapidly on behalf of the local field produced just by the Ising spins. With this in mind, small systematic discrepancies should be expected to occur especially in the region where both $B \to 0$ and $T \to 0$, but, without loss of the qualitative agreement.

Why the Cu1 sites represent a "barrier" for the spin deviations also in the spin-1/2 Heisenberg F-F-AF-AF BAC still remains an open question. Although the origin of this outstanding feature could be naively understood as a general feature of the spins coupled by the F interactions only, this suggestion is in an obvious contradiction with Hida's results for the spin-1/2 F-F-AF BAC.[22] As a matter of fact, the total magnetization of this system varies smoothly with increasing magnetic field even in the ground state, which implies that the spin deviations are delocalized over the whole chain and thus there is a certain quantum reduction also at purely ferromagnetically coupled sites.

A. Survey of theoretical results

In this part, an extensive survey of theoretical results will be presented in order to enable deep insight into the magnetic behavior of the system under investigation. For the sake of simplicity, we shall first suppose equal g factors at the Cu1, Cu2, and Cu3 positions, i.e., $g_1=g_2=g_3=g$.

We start our discussion with the analysis of the ground state. Below some critical external magnetic field, the ground state exhibits an interesting ferrimagnetic order, which can be characterized by the following values of the ground-state magnetization:

$$m_1 = \frac{1}{2}, \quad m_2 = \frac{1}{4}\left[1 + \frac{1 + J_F/J_{AF}}{\sqrt{(1 + J_F/J_{AF})^2 + 8\Delta^2}}\right],$$

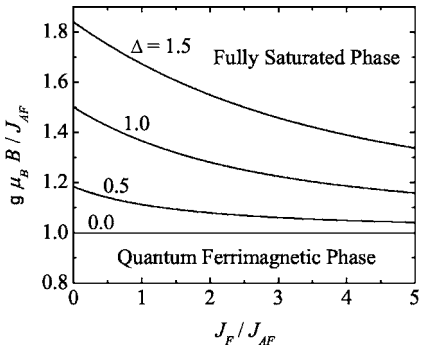

FIG. 3. The ground-state phase diagram in the J_F-B plane obtained for several exchange anisotropies Δ under the assumption of uniform g factors, i.e., $g_1=g_2=g_3=g$.

$$m_3 = -\frac{1}{2}\frac{1 + J_F/J_{AF}}{\sqrt{(1 + J_F/J_{AF})^2 + 8\Delta^2}}, \quad \frac{m}{m_s} = \frac{1}{2}, \tag{25}$$

where m_s labels the saturation magnetization normalized per one Cu^{2+} ion. As already mentioned in the preceding part, the magnetization m_1 retains in the ground state its saturation value in contrast to the magnetization m_2 and m_3, which show obvious quantum reduction. It is quite evident that the stronger the exchange anisotropy Δ, the greater the reduction of the magnetization m_2 and m_3. On the other hand, the quantum reduction of the magnetization completely vanishes in the Ising limit $\Delta \to 0$, when the ground state exhibits a "classical" ferrimagnetic order $\uparrow\uparrow\downarrow\uparrow\cdots$ (Cu1Cu2Cu3Cu2$\cdots$) of a rather trivial nature.

As expected, the ferrimagnetic system undergoes a field-induced metamagnetic transition toward the fully saturated phase under the certain magnetic field. It can be readily proved that the transition field B_t is given by the condition

$$g\mu_B B_t/J_{AF} = \frac{1}{4}(3 - J_F/J_{AF} + \sqrt{(1 + J_F/J_{AF})^2 + 8\Delta^2}). \tag{26}$$

For illustration, Fig. 3 displays the ground-state phase diagram in the J_F-B plane for several values of the exchange anisotropy Δ. As one can see, increasing strength of the F coupling J_F generally reinforces the gradual decline of the transition field. Thereby, the pure Ising limit ($\Delta=0$) represents the only exceptional case when the magnitude of the transition field does not change as the ratio J_F/J_{AF} varies. It can be easily understood that the metamagnetic transition arises in this particular case from a single flip of the central (Cu3) spin of each AF trimer, which occurs when the exchange energy of J_{AF} is thoroughly balanced by the external magnetic field ($g\mu_B B_t=J_{AF}$).

The situation becomes much more complex on considering the nonzero exchange anisotropy Δ. Due to the quantum fluctuations, the spin oriented in the opposite direction with respect to the external field is no longer rigidly connected with the central spin of the AF trimer, but is collectively held by the entire trimer. In other words, the reversed spin is delocalized over the whole AF trimer and consequently there is a nonzero probability that the side (Cu2) spins of the trimer are aligned opposite to the field direction. Naturally, this

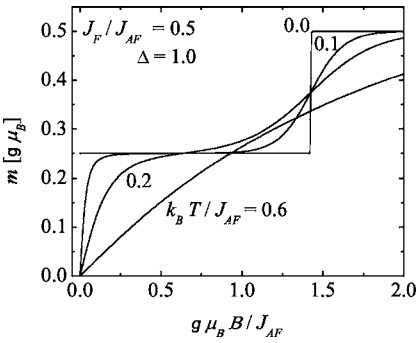

FIG. 4. The total magnetization scaled in $g\mu_B$ units as a function of the dimensionless magnetic field $g\mu_B B/J_{AF}$ for $J_F/J_{AF}=0.5$, $\Delta=1.0$, and several dimensionless temperatures $k_B T/J_{AF}$.

must lead to the enhancement of the exchange energy between the ferromagnetically coupled Cu2 side spins and the fully polarized Cu1 spins. In consequence of that, it is quite conspicuous that the suppression of the transition field can be explained in terms of the energetic destabilization of the quantum ferrimagnetic order, which occurs when J_F/J_{AF} increases.

Now, let us turn our attention to the magnetic behavior at finite temperatures. In Fig. 4 we plot the total magnetization scaled in $g\mu_B$ units against the dimensionless magnetic field ($g\mu_B B/J_{AF}$) for a few temperatures. It should be pointed out that the magnetization curve starts at any finite temperature from zero according to the one-dimensional character of the spin system. The sharp stepwise magnetization curve observable in the zero-temperature limit is, however, gradually smeared out as the temperature is raised from zero. Actually, the conversion toward the fully saturated phase does not occur merely at one precise value of the transition field, but is smudged over a finite range of the fields. In addition, the temperature-induced fluctuations greatly shrink also the width of the magnetization plateau and above a certain temperature the plateau state completely disappears from the magnetization curve. By any means, Fig. 4 provides further convincing evidence that the observed magnetization plateau emerges, under the assumption of uniform g factors, exactly at one-half of the saturation magnetization [see also Eq. (25)].

The variation of the field-induced magnetization with the temperature (Fig. 5) is also interesting on account of the magnetically ordered ground state. At low magnetic fields, the total magnetization tends abruptly to zero as the temperature increases. Nevertheless, one finds here also a noticeable temperature-induced increase of the magnetization within a range of moderate fields, when the total magnetization shows a broad maximum resulting from a vigorous thermal excitations of the Cu3 spins and smaller thermal excitations of the Cu2 spins. However, when the magnetic field exceeds the transition field given by the condition (26), the total magnetization monotonically decreases with increasing temperature as it already starts from its maximum value.

The thermal dependence of the zero-field susceptibility times temperature (χT) data is displayed in Fig. 6. Interestingly, the χT product exhibits a round minimum upon cooling and then diverges under further temperature suppression.

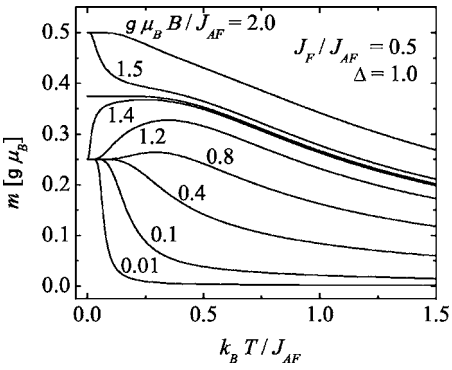

FIG. 5. Some typical temperature variations of the total magnetization obtained for $J_F/J_{AF}=0.5$, $\Delta=1.0$, and several magnetic fields.

As already discussed in several papers concerned with the QFC,[2] a thermal dependence of this type reveals a ferromagnetic-to-antiferromagnetic crossover. Really, the temperature variation of the χT data is in general a monotonically decreasing function for ferromagnets, but monotonically increasing for antiferromagnets. In this respect, the marked low-temperature divergence of the susceptibility emerges because of the gapless F excitations from the magnetically ordered ground state. The position of the round minimum, on the other hand, designates the temperature above which the gapped excitations of the AF nature overhelm the gapless excitations originating from J_F. In accordance with the above statement, the round minimum flattens as the ratio J_F/J_{AF} strengthens and simultaneously its position is shifted toward higher temperatures.

As far as the magnetic susceptibility at nonzero fields is concerned (Fig. 7), the χT always initiates from zero because of the energy gap opened by the magnetic field. However, the thermal dependence of the χT data shows at weak fields a dramatic increase until it reaches a sharp maximum, which is followed by the familiar round minimum of the same origin, as already discussed by the zero-field susceptibility. The appearance of the additional sharp peak can obviously be related to thermal instability of the magnetically ordered system, because already a small temperature change necessitates a huge variation of the magnetization at low fields (see Fig. 5). As a matter of fact, the χT product rises steadily with the

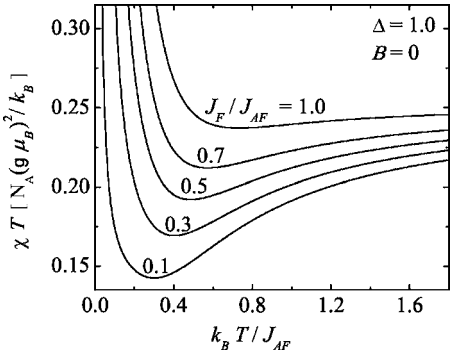

FIG. 6. The thermal dependence of the zero-field susceptibility times temperature data scaled in $N_A(g\mu_B)^2/k_B$ units (N_A is Avogadro's number) for $\Delta=1.0$ and some typical values of J_F/J_{AF}.

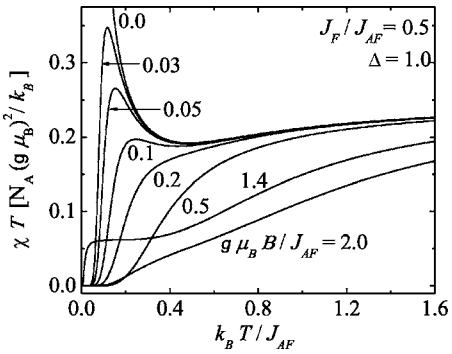

FIG. 7. The temperature dependence of the χT product as a function of the field strength when $J_F/J_{AF}=0.5$ and $\Delta=1.0$.

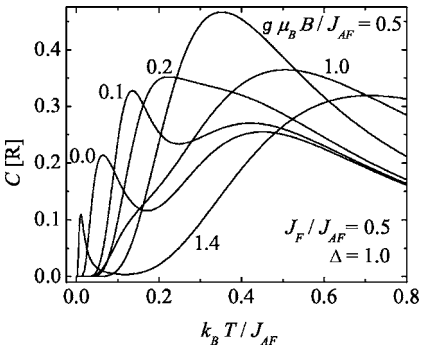

FIG. 9. The thermal dependence of the specific heat by various magnitudes of the external magnetic field when $J_F/J_{AF}=0.5$ and $\Delta=1.0$.

temperature at sufficiently strong fields, since the thermal fluctuations are not strong enough to induce a simultaneous excitation of a large number of spins. Thus, an interesting thermal dependence of the susceptibility appears for strong magnetic fields just around the transition to the fully polarized state. Under these circumstances, the T-χT plot exhibits a rapid increase over a small temperature range, which is subsequently followed by a narrow plateau that continuously passes into a slowly repeating increase of the susceptibility (see the curve $g\mu_B B/J_{AF}=1.4$).

To receive a complete picture of the thermodynamics, the thermal variations of the specific heat are plotted in Figs. 8 and 9. When considering the zero-field case (Fig. 8), the specific heat displays as a function of the temperature a remarkable double-peak structure. There are strong indications that the first sharper peak observed at lower temperature originates from the F excitations: the peak becomes wider as the ratio J_F/J_{AF} increases and is shifted to higher temperatures notwithstanding its almost constant height. Under the assumption of dominant F coupling constant ($J_F/J_{AF}>1.0$), the low-temperature peak is to a large extent superimposed on the second broader maximum that occurs at a little bit higher temperature. Obviously, the round high-temperature maximum can be thought of as the usual Schottky-type maximum, which has a tendency to be enhanced in magnitude with increasing J_F/J_{AF}. When comparing the results displayed in Fig. 8 with those of the pure Heisenberg F-F-AF-AF BAC obtained using the exact diagonalization method[27] or the transfer-matrix renormalization group,[32] an excellent agreement is found as far as the high-temperature maxima of both these models are concerned. The only difference thus rests in the height of the low-temperature peak which is, due to the Ising approximation of J_F, roughly three times higher for the Ising-Heisenberg BAC compared to that of the pure Heisenberg BAC (see, for instance, the inset of Fig. 4 depicted in Ref. 32).

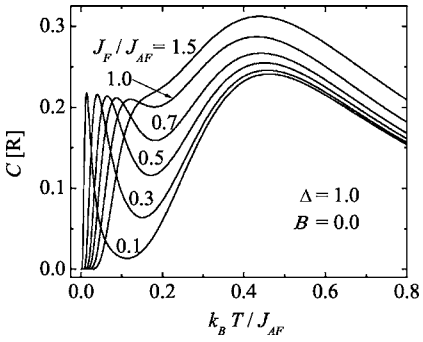

FIG. 8. The zero-field specific heat as a function of the temperature for some typical values of J_F/J_{AF} and $\Delta=1.0$. The specific heat is scaled in multipliers of the universal gas constant $R=8.314\ \mathrm{J\ K^{-1}\ mol^{-1}}$.

The situation becomes even more interesting on applying a magnetic field (Fig. 9). The effect of a small magnetic field is to increase the height of the low-temperature peak and to move it toward higher temperatures (see the case $g\mu_B B/J_{AF}=0.1$). This result is taken to mean that under a certain field both maxima coalesce and consequently the specific heat exhibits a single nonrounded maximum as shown for $g\mu_B B/J_{AF}=0.2$. By an additional increase of the field strength, the specific heat curve gradually loses its irregular profile and the overall trend is that the Schottky-type maximum drops in magnitude and moves to higher temperatures. Apart from this rather trivial finding, the double-peak specific heat curve can be recovered for the fields close to the transition to the fully saturated phase (e.g., $g\mu_B B/J_{AF}=1.4$). It should be mentioned, however, that the height of the low-temperature peak is in this case considerably smaller than that of the zero-field specific heat. Although the external field spreads also this low-temperature peak until it completely merges with the Schottky-type maximum, the change of the peak position occurs strikingly without any significant change of the peak height (for clarity, this effect is not shown here). Finally, it should be stressed that the observed behavior of the specific heat is not a generic feature of the special class of the Ising-Heisenberg BAC; nevertheless, it has already been recognized also in the pure Ising BAC (compare with Figs. 4 and 8 in Ref. 37).

We conclude our survey of the thermodynamic properties by considering the nonuniformity of the g factors at the structurally and therefore also magnetically nonequivalent Cu1, Cu2, and Cu3 positions (i.e., $g_1\neq g_2\neq g_3$). Let us first focus on the ground-state behavior. The most interesting finding to emerge here is that the ground-state magnetization

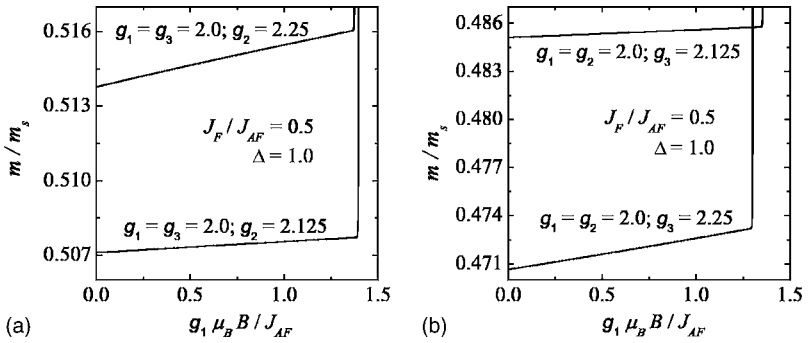

FIG. 10. The field variation of the ground-state magnetization normalized with respect to its saturation value by assuming the nonuniformity of the g factors. (a) [(b)] shows the situation when $g_2 > g_1 = g_3$ [$g_3 > g_1 = g_2$].

depend on the field strength, whenever $g_2 \neq g_3$:

$$m_1 = \frac{1}{2},$$

$$m_2 = \frac{1}{4}\left\{1 + \frac{1 + J_F/J_{AF} + 2\mu_B B(g_2 - g_3)/J_{AF}}{\sqrt{[1 + J_F/J_{AF} + 2\mu_B B(g_2 - g_3)/J_{AF}]^2 + 8\Delta^2}}\right\},$$

$$m_3 = -\frac{1}{2}\frac{1 + J_F/J_{AF} + 2\mu_B B(g_2 - g_3)/J_{AF}}{\sqrt{[1 + J_F/J_{AF} + 2\mu_B B(g_2 - g_3)/J_{AF}]^2 + 8\Delta^2}},$$

$$\frac{m}{m_s} = \frac{g_1 + g_2}{g_1 + 2g_2 + g_3} + \frac{g_2 - g_3}{g_1 + 2g_2 + g_3} \times \frac{1 + J_F/J_{AF} + 2\mu_B B(g_2 - g_3)/J_{AF}}{\sqrt{[1 + J_F/J_{AF} + 2\mu_B B(g_2 - g_3)/J_{AF}]^2 + 8\Delta^2}}. \quad (27)$$

It is quite apparent from Eqs. (27) that the field dependence of the total magnetization comes from the corresponding field variations of the on-site magnetization m_2 and m_3. Another noticeable feature to observe here is that the magnetic field suppresses (raises) the quantum reduction of the magnetization m_2 and m_3 as long as $g_2 > g_3$ ($g_2 < g_3$). Since the condition $2\mu_B B(g_2 - g_3) \ll J_F + J_{AF}$ holds for most of the experimentally accessible fields and g factors, the total magnetization should be nearly linearly dependent on the magnetic field with a linear term proportional to the difference $\delta g = g_2 - g_3$. Naturally, the greater the magnitude of the external field and δg, the stronger deviations from the linearity should emerge.

Some typical examples of the ground-state magnetization curves are depicted in Fig. 10 under the assumption $g_2 > g_1 = g_3$ [Fig. 10(a)] and $g_3 > g_1 = g_2$ [Fig. 10(b)]. These results can serve as evidence that the magnetization curve does not show an exact plateau, but rises steadily with the external field. It is also worthy of note that these "magnetization plateaus with a finite slope" (when plotted in the full range with respect to the saturation magnetization, they are hardly discernible from the exact plateaus within reasonable values of the g factors) do not occur precisely at half of the saturation magnetization ($m/m_s = 1/2$), but they are shifted to higher values if $g_2 > g_1 = g_3$ [Fig. 10(a)] and to smaller values if $g_3 > g_1 = g_2$ [Fig. 10(b)].

To enable an independent check of the field dependence of the total magnetization, the temperature variation of the susceptibility has been examined in detail. The typical thermal dependences of the susceptibility are plotted in Fig. 11 for $g_3 > g_1 = g_2$ and some selected external fields. Generally, the susceptibility versus temperature plot can be characterized by a round maximum, which flattens and shifts to higher temperatures when increasing the external field. The low-temperature part of the susceptibility is displayed on an enlarged scale in the inset. It turns out that the susceptibility does not completely vanish as the temperature approaches zero; nevertheless, it tends toward a small but finite value. This result provides a confirmation of the striking field-dependent magnetization and moreover it also clearly demonstrates a gapless excitation spectrum above the ground state.

B. Comparison with the experimental data

At this stage, the results obtained from the exact mapping on the Ising-Heisenberg BAC will be compared with the available experimental data for a single-crystal sample of the CCPA. It should be mentioned here that all the experimental data used in our further analysis have already been reported in earlier publications[26,27] to which the interested reader is referred for more experimental details.

In order to fit the experimental data of the CCPA, we have to consider six fitting parameters: the exchange constant J_{AF}/k_B, the exchange anisotropy Δ, the alternation ratio J_F/J_{AF}, and the three g factors g_1, g_2, and g_3. Note that the best fit of the magnetization and the susceptibility data obtained under the restriction of equal g factors ($g_1 = g_2 = g_3$) as well as isotropic exchange J_{AF} ($\Delta = 1.0$) have already been

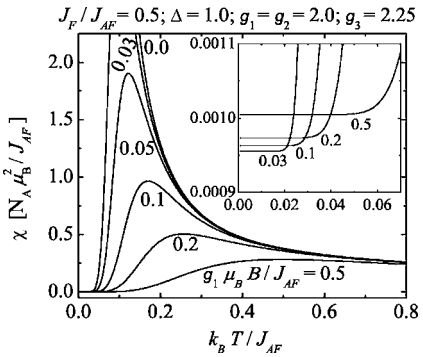

FIG. 11. The temperature dependence of the susceptibility when varying the external field strength, and $J_F/J_{AF} = 0.5$, $\Delta = 1.0$, $g_1 = g_2 = 2.0$, and $g_3 = 2.25$. The inset displays the low-temperature susceptibility on an enlarged scale.

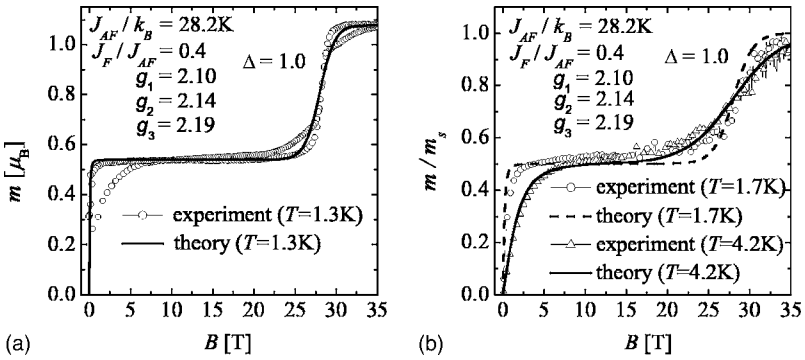

FIG. 12. The low-temperature magnetization curves measured in pulsed (a) and static (b) magnetic fields together with the corresponding theoretical prediction obtained for this fitting set of parameters: J_{AF}/k_B=28.2 K, J_F/J_{AF}=0.4, Δ=1.0, g_1=2.10, g_2=2.14, and g_3=2.19. The hysteresis observed in the experimental curves near zero and saturation fields is probably caused by the magnetocaloric effect.

published by the present authors in our preliminary report (see Fig. 3 in Ref. 30). Unless specifically mentioned, the exchange anisotropy will again be fixed to the purely isotropic case Δ=1.0, because the experimental measurements on the single-crystal sample do not reveal any significant spatial dependence: the spatial directions parallel and perpendicular to the chain axis seem to be almost equivalent.[26]

In Fig. 12, the low-temperature magnetization curve of CCPA measured in the pulsed [Fig. 12(a)] and static [Fig. 12(b)] magnetic fields is compared with the relevant theoretical prediction (the fitting parameters are indicated in the figures). It turns out, however, that the average g factor must be approximately $g_{av} \equiv (g_1+2g_2+g_3)/4 \sim 2.15$ in order to get the correct saturation magnetization [Fig. 12(a)]. Even under this confinement, several combinations of the g factors provide almost the same fit to the experimental magnetization curve. For illustrative purposes, we choose the one with the smallest value of the g_1 factor to lower the susceptibility of the Cu1 spins, because the most obvious discrepancies between the theory and the experiment emerge near zero field due to the more susceptible character of the Ising spins, as already discussed earlier.

Unfortunately, it is beyond experimental verification to find out from the existing data set whether the magnetization increase observed within the plateau region appears exclusively on account of the finite-temperature effect, or is partially caused by the inequality $g_2 \neq g_3$. Although the former situation cannot be definitely ruled out, it is rather more acceptable that there is at least a small contribution to the magnetization increase also from the difference between the g factors. Nonetheless, the final conclusion is complicated by different factors: the magnetization curves in the static fields [Fig. 12(b)] are measured at higher temperatures and become quite noisy above 15 T, while the available magnetization curve in the pulsed fields [Fig. 12(a)] show a relatively large hysteresis probably caused by the magnetocaloric effect.[26]

The thermal dependence of the zero-field susceptibility times temperature data is illustrated in Fig. 13. To obtain a reasonable accordance with the experimental measurement, slightly higher g factors must be taken into consideration in comparison with the ones acquired by the fitting of the magnetization. Despite this fact, a quite impressive accordance can be achieved by rescaling the average g factor at about 4–5 % of its magnetization value $g_{av} \sim 2.15$. As expected, the most apparent disagreement appears in the descending tail of the χT curve near zero temperature, where the susceptibility divergence is reminiscent of the ferromagnetic Ising-type divergence rather than the Heisenberg-type divergence.

Finally, Fig. 14 shows the magnetic part of the specific heat as a function of the temperature for several magnetic fields. The corresponding theoretical predictions are also included; nevertheless, the specific heat can only be fitted with a rather unacceptable precision even though the results agree at least qualitatively. In order to situate the striking low-temperature peak around 0.5 K, however, a drastic reduction of the J_F and J_{AF} exchange parameters was carried out. Even under this condition, the predicted peak is much more robust than observed experimentally and this feature remains valid also for any other combination of the J_F and J_{AF} coupling constants. Actually, the height of the low-temperature peak does not significantly vary with the ratio J_F/J_{AF} as already shown in Fig. 8.

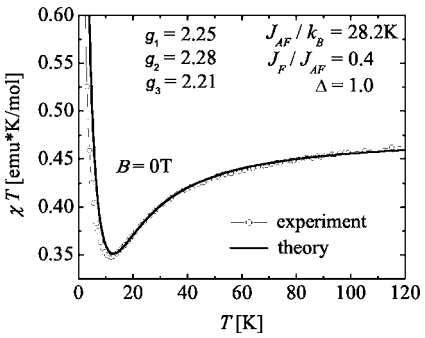

FIG. 13. The zero-field susceptibility times temperature data and the corresponding theoretical prediction (the fitting parameters are indicated in the figure).

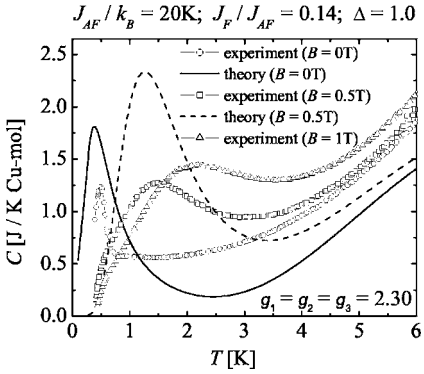

FIG. 14. The thermal dependence of the specific heat measured at B=0.0, 0.5, and 1.0 T. The corresponding theoretical predictions are also included.

It is quite obvious that the inconsistency in the fitting set for the specific heat and, respectively, the magnetization and susceptibility, indicates some insufficiency in the considered model based on the simple concept of the F-F-AF-AF BAC. Notice that the basic problem that prevents obtaining a unique fitting set for all these quantities consists in reproducing the striking low-temperature peak of the specific heat, which cannot be fitted within a reasonable accord under the assumption of the pure Heisenberg F-F-AF-AF BAC.[27,32] A possible explanation for this peculiar inconsistency has recently been suggested by Lu *et al.*,[32] who found a strong indication that the striking low-temperature peak comes from the contribution of magnetic impurities. Until a higher-quality sample of CCPA is remeasured, however, one cannot exclude the other possibility that this anomalous peak originates from the neglected higher-order interaction terms in the proposed Hamiltonian. Our detailed analysis shows that neither the nonuniformity of g factors nor the exchange anisotropy of the $J_{AF}(\Delta)$ coupling constant can resolve this inconsistency.

IV. CONCLUDING REMARKS

In the present article, the magnetic properties of the spin-1/2 Ising-Heisenberg chain with regular F-F-AF-AF bond alternation have been investigated within the exact mapping transformation method. The results obtained from the mapping procedure are compared with the results of the corresponding Heisenberg BAC,[26] and with the experimental data of the CCPA compound,[26,27] which is regarded to be an experimental realization of the spin-1/2 F-F-AF-AF BAC.

It should be emphasized that all characteristic quantum features observed[25–27] in the spin-1/2 Heisenberg F-F-AF-AF BAC are still present also in our simplified Ising-Heisenberg version: one finds here a substantial quantum reduction of the ground-state magnetization m_2 and m_3 at the Cu2 and Cu3 sites in addition to the fully saturated ground-state magnetization m_1 at the Cu1 site. Perhaps the most striking finding stemming from our study is that there appears a rather unusual change from the gapful to gapless excitation spectrum when converting the uniform g factors at structurally nonequivalent positions to nonuniform ones. With regard to this, the magnetization curve exhibits a real plateau under the condition $g_2=g_3$ only; for any other case the magnetization within the quantum ferrimagnetic phase (plateau state) shows a weak field dependence.

The success of the simplified Ising-Heisenberg model in reproducing the measured data for CCPA is also quite remarkable. With the exception of the specific heat, where the results agree at the qualitative level only, other thermodynamic quantities are relatively well reproduced. In fact, small systematic errors occur merely in the low-temperature and weak-field region, where the approximation of the ferromagnetic coupling J_F by the Ising-type interaction plays the most essential role. It is worthwhile to mention, moreover, that the discrepancy found in the specific heat fit cannot be resolved even if a pure Heisenberg F-F-AF-AF BAC is considered. Actually, very recent work of Lu *et al.*[32] provided a strong indication that the striking low-temperature peak of specific heat is of extrinsic origin probably caused by the presence of magnetic impurities. However, further experimental measurements with high-quality samples of CCPA are required to clarify this issue. Finally, one should notice that the simple concept of the Ising-Heisenberg F-F-AF-AF BAC presented here can be rather straightforwardly extended to account for second-neighbor interactions, the antisymmetric Dzyaloshinsky-Moriya interaction, and/or multispin interactions, which cannot be ruled out as a potential cause of the observed discrepancies until the influence of magnetic impurities is experimentally confirmed.

ACKNOWLEDGMENTS

One of the authors (J.S.) would like to thank Dr. M. Jurčišin and Professor N. M. Plakida for their kind hospitality during his stay at the Joint Institute for Nuclear Research (JINR) in Dubna, where part of this work was completed. The author is also indebted to Professor J. Richter and Dr. V. N. Plechko for fruitful discussions and valuable suggestions. One of the authors (M.H.) expresses his sincere thanks to Dr. H. A. Katori, Dr. H. Kitazawa, Dr. H. Suzuki, Dr. N. Tsujii, and Dr. H. Abe for their help in performing the experiments. Some of the experimental work was done under the Visiting Researcher Program of KYOKUGEN at Osaka University. This work was partially (J.S. and M.J.) supported under Grant No. VEGA 1/2009/05 and APVT-20-005204.

*Electronic address: jozkos@pobox.sk

[1] S. K. Pati, S. Ramasesha, and D. Sen, J. Phys.: Condens. Matter **9**, 8707 (1997); Phys. Rev. B **55**, 8894 (1997); F. C. Alcaraz and A. L. Malvezzi, J. Phys. A **30**, 767 (1997).

[2] A. K. Kolezhuk, H.-J. Mikeska, and S. Yamamoto, Phys. Rev. B **55**, R3336 (1997); S. Yamamoto, T. Fukui, K. Maisinger, and U. Schollwöck, J. Phys.: Condens. Matter **10**, 11033 (1998); S. Yamamoto and T. Fukui, Phys. Rev. B **57**, R14008 (1998); K. Maisinger, U. Schollwöck, S. Brehmer, H.-J. Mikeska, and S. Yamamoto, *ibid.* **58**, R5908 (1998); S. Yamamoto and T. Sakai, J. Phys.: Condens. Matter **11**, 5175 (1999).

[3] M. Steiner, J. Villain, and C. G. Windsor, Adv. Phys. **25**, 88 (1976); M. Verdaguer, A. Gleizes, J. P. Renard, and J. Seiden, Phys. Rev. B **29**, 5144 (1984); Y. Pei, M. Verdaguer, O. Kahn, J. Sletten, and J. P. Renard, Inorg. Chem. **26**, 138 (1987); O. Kahn, Y. Pei, M. Verdaguer, J. P. Renard, P. Rey, and J. Sletten, J. Am. Chem. Soc. **110**, 782 (1988); E. Coronado, M. Drillon, P. R. Nugteren, L. J. de Jongh, and D. Beltran, *ibid.* **110**, 3907 (1988); P. J. Van Koningsbruggen, O. Kahn, K. Nakatani, Y. Pei, J. P. Renard, M. Drillon, and P. Leggol, Inorg. Chem. **29**, 3325 (1990); Y. Baron, B. Guillou, J. Sletten, C. Mathoniére, E. Codjovi, and O. Kahn, Inorg. Chim. Acta **235**, 69 (1995); M. Ohba, N. Usuki, N. Fukita, and H. Okawa, Inorg. Chem. **37**, 3349 (1998).

[4] M. Hagiwara, Y. Narumi, K. Minami, K. Tatani, and K. Kindo, J. Phys. Soc. Jpn. **67**, 2209 (1998); **68**, 2214 (1999); N. Fujiwara and M. Hagiwara, Solid State Commun. **113**, 433 (2000).

[5] C. Ruiz-Pérez, J. Sanchiz, M. Hernández-Molina, F. Floret, and M. Julve, Inorg. Chim. Acta **298**, 202 (2000).

[6] E. Pytte, Phys. Rev. B **10**, 4637 (1974); M. C. Cross and D. S. Fisher, *ibid.* **19**, 402 (1979).

[7] M. Hase, I. Terasaki, and K. Uchinokura, Phys. Rev. Lett. **70**, 3651 (1993); M. Hase, I. Terasaki, Y. Sasago, K. Uchinokura, and H. Obara, *ibid.* **71**, 4059 (1993); M. C. Martin, G. Shirane, Y. Fujii, M. Nishi, O. Fujita, J. Akimitsu, M. Hase, and K. Uchinokura, Phys. Rev. B **53**, R14713 (1996); S. Sahling, G. Reményi, J. C. Lasjaunias, N. Hegman, G. Dhalenne, and A. Revcolevschi, Physica B **219-220**, 110 (1996).

[8] M. Isobe and Y. Ueda, J. Phys. Soc. Jpn. **65**, 1178 (1996); M. Weiden, R. Hauptmann, C. Geibel, F. Steglich, M. Fischer, P. Lemmens, and G. Güntherodt, Z. Phys. B: Condens. Matter **103**, 1 (1997); M. Weiden, R. Hauptmann, C. Geibel, M. Köppen, J. Müller, M. Lang, F. Steglich, N. Weiden, M. Fischer, P. Lemmens, and G. Güntherodt, J. Magn. Magn. Mater. **171-181**, 743 (1998).

[9] D. Guo, T. Kennedy, and S. Mazumdar, Phys. Rev. B **41**, 9592 (1990); M. Roji and S. Miyashita, J. Phys. Soc. Jpn. **65**, 1994 (1996); T. Tonegawa, T. Nakao, and M. Kaburagi, *ibid.* **65**, 3317 (1996); F. Schönfeld, G. Bouzerar, G. S. Uhrig, and E. Müller-Hartmann, Eur. Phys. J. B **5**, 521 (1998); M. Saito and H. Fukuyama, J. Phys. Chem. Solids **60**, 1113 (1999); Q. Jiang, X. Y. Chen, and X. F. Jiang, Phys. Lett. A **287**, 397 (2001).

[10] F. D. M. Haldane, Phys. Lett. **93A**, 464 (1983); Phys. Rev. Lett. **50**, 1153 (1983).

[11] M. Yamashita, T. Ishii, and H. Matsuzaka, Coord. Chem. Rev. **198**, 347 (2000).

[12] K. Hida, Phys. Rev. B **45**, 2207 (1992); **46**, 8268 (1992); J. Phys. Soc. Jpn. **62**, 1463 (1993).

[13] M. Kohmoto and H. Tasaki, Phys. Rev. B **46**, 3486 (1992); M. Yamanaka, Y. Hatsugai, and M. Kohmoto, *ibid.* **48**, 9555 (1993); K. Okamoto, D. Nishino, and Y. Saika, J. Phys. Soc. Jpn. **62**, 2587 (1993); K. Okamoto, J. Phys. A **29**, 1639 (1996).

[14] I. Vasilevesky, N. R. Rose, R. Stenkamp, and R. D. Willett, Inorg. Chem. **30**, 4082 (1991); J. J. Borrás-Almenar, E. Coronado, J. Curely, R. Georges, and J. C. Gianduzzo, *ibid.* **33**, 5171 (1994); M. Hagiwara, Y. Narumi, K. Kindo, T. C. Kobayashi, H. Yamakage, K. Amaya, and G. Schumauch, J. Phys. Soc. Jpn. **66**, 1792 (1997).

[15] L. P. Battaglia, A. B. Corradi, G. Marcotrigiano, L. Menabue, and G. C. Pellacani, Inorg. Chem. **19**, 125 (1980); H. J. M. de Groot, L. J. de Jongh, and R. D. Willett, J. Appl. Phys. **53**, 8038 (1982); S. O'Brien, R. M. Gaura, C. P. Landee, B. L. Ramakhrishna, and R. D. Willett, Inorg. Chim. Acta **141**, 83 (1988); M. Hagiwara, Y. Narumi, K. Kindo, T. C. Kobayashi, H. Yamakage, K. Amaya, and G. Schumauch, J. Phys. Soc. Jpn. **66**, 1792 (1997).

[16] H. Manaka, I. Yamada, and K. Yamaguchi, J. Phys. Soc. Jpn. **66**, 564 (1997); H. Manaka and I. Yamada, J. Magn. Magn. Mater. **177-181**, 681 (1998).

[17] R. D. Willet, J. Chem. Phys. **44**, 39 (1966); S. Lahiri and R. Kakkar, Chem. Phys. Lett. **78**, 379 (1981); Y. Ajiro, K. Takeo, Y. Inagaki, T. Asano, A. Shimogai, M. Mito, T. Kawae, K. Takeda, T. Sakom, and H. Nojiri, Physica B **329-333**, 1008 (2003).

[18] G. De Munno, M. G. Lombardi, M. Julve, F. Lloret, and J. Faus, Inorg. Chim. Acta **282**, 82 (1998).

[19] A. Escuer, M. Font-Bardía, E. Peñalba, X. Solans, and R. Vicente, Polyhedron **18**, 211 (1999).

[20] T. K. Maji, P. S. Mukherjee, S. Koner, G. Mostafa, J.-P. Tuchagues, and N. R. Chaudhuri, Inorg. Chim. Acta **314**, 111 (2001).

[21] M. Oshikawa, M. Yamanaka, and I. Affleck, Phys. Rev. Lett. **78**, 1984 (1997); I. Affleck, Phys. Rev. B **37**, 5186 (1998).

[22] K. Hida, J. Phys. Soc. Jpn. **63**, 2359 (1994); K. Okamoto, Solid State Commun. **98**, 245 (1996); A. Kitazawa and K. Okamoto, J. Phys.: Condens. Matter **11**, 9765 (1999); K. Okamoto and A. Kitazawa, Physica B **281-282**, 840 (2000).

[23] J. C. Livermore, R. D. Willett, R. M. Gaura, and C. P. Landee, Inorg. Chem. **21**, 1403 (1982); Y. Ajiro, T. Asano, T. Inami, H. Aruga-Katori, and T. Goto, J. Phys. Soc. Jpn. **63**, 859 (1994); T. Goto, Y. Ajiro, T. Asano, T. Inami, and H. Aruga-Katori, Physica B **216**, 294 (1996).

[24] A. Escuer, R. Vicente, M. S. El Fallah, M. A. S. Goher, and F. A. Mautner, Inorg. Chem. **37**, 4466 (1998).

[25] M. Hagiwara, Y. Narumi, K. Minami, and K. Kindo, Physica B **294-295**, 30 (2001).

[26] M. Hagiwara, Y. Narumi, K. Minami, K. Kindo, H. Kitazawa, H. Suzuki, N. Tsujii, and H. Abe, J. Phys. Soc. Jpn. **72**, 943 (2003).

[27] M. Hagiwara, K. Minami, and H. A. Katori, Prog. Theor. Phys. Suppl. **145**, 150 (2003).

[28] M. Hagiwara, in *EPR in the 21st Century*, edited by A. Kawamori, J. Yamauchi, and H. Ohta (Elsevier Science, Amsterdom, 2002), pp. 73–78.

[29] L. K. Thompson, S. S. Tandon, and M. E. Manuel, Inorg. Chem. **34**, 2356 (1995).

[30] J. Strečka, M. Hagiwara, M. Jaščur, and K. Minami, Czech. J. Phys. **54**, D583 (2004).

[31] I. Syozi, in *Phase Transitions and Critical Phenomena*, edited by C. Domb and M. S. Green (Academic Press, New York, 1972), Vol. 1, pp. 269–329; M. E. Fisher, Phys. Rev. **113**, 969 (1959).

[32] We recently received work dealing with the spin-1/2 Heisenberg F-F-AF-AF BAC treated within the transfer-matrix renormalization group [H. T. Lu, Y. H. Su, L. Q. Sun, J. Chang, C. S. Liu, H. G. Luo, and T. Xiang, cond-mat/0412275 (unpublished)].

[33] J. Strečka and M. Jaščur, Czech. J. Phys. **52**, A37 (2002); J. Phys.: Condens. Matter **15**, 4519 (2003).

[34] M. Jaščur and J. Strečka, J. Magn. Magn. Mater. **272-276**, 984 (2004); L. Čanová, J. Strečka, and M. Jaščur, Czech. J. Phys. **54** (2004) D579.

[35] J. Strečka and M. Jaščur, Phys. Rev. B **66**, 174415 (2002); Phys. Status Solidi B **233**, R12 (2002); M. Jaščur and J. Strečka, Acta Electrotech. Informatica **2**, 71 (2002); J. Strečka and M. Jaščur, J. Magn. Magn. Mater. **272-276**, 987 (2004); M. Jaščur and J. Strečka, Czech. J. Phys. **54**, D587 (2004).

[36] E. Ising, Z. Phys. **31**, 253 (1925); D. A. Lavis and G. M. Bell, *Statistical Mechanics of Lattice Systems* (Springer, Berlin, 1999), Vol. 1.

[37] K. Minami, J. Phys. Soc. Jpn. **67**, 2255 (1998).